

# Microwave Triggered Metal Enhanced Chemiluminescence: Quantitative Protein Determination

Michael J. R. Previte,<sup>†</sup> Kadir Aslan,<sup>†</sup> Stuart N. Malyn,<sup>†</sup> and Chris D. Geddes<sup>\*†‡</sup>

*Institute of Fluorescence, Laboratory for Advanced Medical Plasmonics, Medical Biotechnology Center, University of Maryland Biotechnology Institute, 725 West Lombard Street, Baltimore, Maryland 21201, and Center for Fluorescence Spectroscopy, Medical Biotechnology Center, University of Maryland School of Medicine, 725 West Lombard Street, Baltimore, Maryland 21201*

We present a new technology that offers a faster alternative to the chemiluminescence-based detection that is used in protein assay platforms today. By combining the use of silver nanostructures with chemiluminescent species, a technique that our laboratories have recently shown can enhance the system photon flux over 50-fold, with the use of low-power microwave heating to additionally accelerate, in essence “trigger”, chemiluminescence-based reactions, then both ultrafast and ultrabright chemiluminescence assays can be realized. In addition, the preferential heating of the nanostructures by microwaves affords for microwave triggered metal enhanced chemiluminescence (MT-MEC) to be localized in proximity to the silvered surfaces, alleviating unwanted emission from the distal solution. To demonstrate MT-MEC, we have constructed a model assay sensing platform on both silvered and glass surfaces, where comparison with the identical glass substrate-based assay serves to confirm the significant benefits of using silver nanostructures for metal-enhanced chemiluminescence. Our new model assay technology can detect femtomoles of biotinylated BSA in less than 2 min and can indeed be modified to both detect and quantify a great many other biomolecules as well. As compared to traditional western blot approaches, MT-MEC offers protein quantification, high-sensitivity detection combined with ultrafast assay times, i.e., <2 min.

There is an increasing demand for the use of light-producing chemical reactions for quantitative detection in biotechnology, especially with regard to chemiluminescence-based ligand-binding assays.<sup>1</sup> The attractiveness of chemiluminescence as an analytical tool lies primarily in the simplicity of detection,<sup>2</sup> since most samples have no unwanted background luminescence and no optical filters are required to separate the excitation wavelengths and scatter.<sup>2</sup> In this regard, luminol and lucigenin (the more

common derivatives being acridan) are used extensively throughout biological research and clinical testing for diagnostic purposes, e.g., the western blot.<sup>3,4</sup> The analytical applications commonly include immunoassays, antioxidant assays, microbiology, protein blotting, nucleic acid analysis, cellular studies, cancer detection, and disease screening.<sup>5</sup>

Although diverse families of immunoassays are widely used for the detection and determination of a wide variety of proteins, peptides and small molecules,<sup>3–8</sup> perhaps, one of the most commonly practiced methodologies is the western blot.<sup>3,4</sup> These assays typically use antigen–antibody binding for analyte recognition and fluorescence,<sup>6</sup> radioactive<sup>7</sup> or chemiluminescence<sup>8</sup> based readout for signal transduction. Fluorescent-based detection methods have the advantage of protein quantification because detected fluorescent signal is directly proportional to fluorescently labeled species.<sup>9</sup> In addition, analyte detection can be multiplexed using spectrally distinct fluorescently labeled proteins.<sup>9</sup> Fluorescence techniques are limited as additional costly detection equipment is often required, external excitation sources are necessary to induce the photon emission, and limited sensitivity exists at low analyte concentrations.<sup>10</sup>

Autoradiography is another method of protein detection and considered advantageous because of its specificity and sensitivity (5 pg of protein).<sup>11</sup> On the other hand, sensitivity is strongly dependent on often long-exposure conditions (>24 h), labeling efficiencies, and the identity of a radiolabeled probe.<sup>11</sup> Radiolabeling also suffers from inherent disadvantages such as health

\* To whom correspondence should be addressed. E-mail: geddes@umbi.umd.edu.

<sup>†</sup> University of Maryland Biotechnology Institute.

<sup>‡</sup> University of Maryland School of Medicine.

(1) Bronstein, I.; Martin, C. S.; Fortin, J. J.; Olesen, C. E.; Voyta, J. C. *Clin. Chem.* **1996**, *42*, 1542–1546.

(2) Nieman, T. In *Encyclopedia of Analytical Science*; Academic Press: Orlando, FL, 1995; pp 608–613.

(3) Burnette, W. N. *Anal. Biochem.* **1981**, *112*, 195–203.

(4) Towbin, H.; Staehelin, T.; Gordon, J. *Proc. Natl. Acad. Sci. U.S.A.* **1979**, *76*, 4350–4354.

(5) Kricka, L. J. In *Bioluminescence and Chemiluminescence, Part C*; Ziegler, M. M., Baldwin, T. O., Eds.; Methods in Enzymology 305; Academic Press: San Diego, CA, 2000; pp 333–345.

(6) Diamandis, E. P.; Christopoulos, T. K.; Bean, C. C. *J. Immunol. Methods* **1992**, *147*, 251–259.

(7) Hunger, H. D.; Schmidt, G.; Flachmeier, C. *Anal. Biochem.* **1994**, *217*, 98–102.

(8) Bronstein, I.; Voyta, J. C.; Murphy, O. J.; Bresnick, L.; Kricka, L. J. *Biotechniques* **1992**, *12*, 748–753.

(9) Lakowicz, J. R. *Principles of Fluorescence Spectroscopy*, 2nd ed.; Kluwer Academic: New York, 1999.

(10) Thompson, R. B., Ed. *Fluorescence Sensors and Biosensors*; CRC Press: Taylor & Francis Group, LLC: Boca Raton FL, 2006.

(11) Osborn, J. In *Life Science News*; Amersham Biosciences: Little Chalfont, Buckinghamshire, UK, 2000; pp 1–4.

and safety risks and the high cost of materials.<sup>11</sup> Chemiluminescent assays have been shown to be as sensitive as radiolabeling without the associated health hazards and cost of materials.<sup>11</sup> Presently, chemiluminescent techniques for horseradish peroxidase and alkaline phosphatase labels have been commercialized and can detect as low as 1–5 pg of protein.<sup>12</sup> Thus, chemiluminescent techniques have become a method of choice for small-molecule detection in more than 20% of clinical laboratories in the United States.<sup>13</sup>

Although chemiluminescence detection has been successfully implemented, the sensitivity and specificity of these reactions require further improvements to facilitate early diagnosis of the prevalence of disease. In addition, most protein detection methodologies, most notably western blotting, are still not reliable methods for accurate quantification of low protein concentrations without investing in high-sensitivity detection schemes.<sup>14</sup> Protein detection methodologies are also limited by antigen–antibody recognition steps that are generally kinetically very slow and require long incubation times; e.g., western blots require processing times in excess of 4 h.<sup>8</sup> However, more recently, a western blotting methodology (One-Step Western Blot Analysis Kit, GenScript Corp.) has been made available that claims protein detection can be performed in less than 1 h, but this method still does not address the need for reliable protein quantification at low protein concentrations. Thus, both the rapidity and sensitivity of small-molecule assays are still critical issues to be addressed to improve assay detection.<sup>15–21</sup>

In the past two decades, the use of microwave radiation has greatly increased for accelerating reactions in synthetic organic chemistry applications,<sup>22–24</sup> in drug delivery,<sup>25</sup> assays,<sup>26–30</sup> and biochemistry.<sup>31–33</sup> Recently, our laboratory has combined the use of metal-enhanced fluorescence (MEF),<sup>34–37</sup> a new technology that

can dramatically increase the quantum yield and photostability of weakly fluorescing species,<sup>34–36</sup> with the use of low-power microwaves to kinetically accelerate assays, a technology that we refer to as MA-MEF. In this paper, we have shown that the degree of avidin binding to biotinylated bovine serum albumin (BSA) surfaces was identical for 30-s microwave heating as compared to 30-min incubation at room temperature.<sup>36</sup> We also observed that the nonspecific background decreased with 30-s microwave incubations versus the commonly used 30-min, room-temperature incubation.<sup>36</sup> In addition, through fluorescence lifetime and fluorescent resonant energy-transfer studies, we demonstrated that low-power microwave heating did not induce protein structural or environmental changes.<sup>36</sup>

We recently demonstrated the acceleration of chemiluminescence reactions with low-power microwaves, which we attribute to localized microwave heating on the surface of the silvered substrate.<sup>37</sup> As a result, an amplified localized photon flux from the chemiluminescent reaction is observed. In this paper, we now describe microwave triggered metal enhanced chemiluminescence (MT-MEC) for protein detection using low-power microwaves to induce the combined effect of a kinetically accelerated binding, increased binding specificity, and accelerated chemiluminescent reactions. We have found that the use of low-power microwaves, in combination with enzymes and chemiluminescent species, demonstrates that significantly faster (<2 min) total quantitative protein detection could be realized today.

## RESULTS AND DISCUSSION

To demonstrate our new approach to protein detection with MT-MEC on silver island films (SiFs), we used commercially available chemiluminescent reagents (acridan and peroxide) from Amersham Biosciences. The model protein assay was constructed with biotinylated BSA surface-modified substrates (SiFs or glass), horseradish peroxidase–streptavidin (HRP–avidin) and chemiluminescent reagents, as demonstrated in Figure 1.

Biotinylated BSA was incubated on silvered or glass substrates for ~1 h. A 1% aqueous BSA solution was subsequently added to minimize nonspecific binding of HRP–streptavidin to the surfaces. HRP–streptavidin was then added to the surfaces with bound biotinylated BSA. The strong binding affinity of streptavidin for biotin served as the basis for the quantitative determination of the BSA–biotin species on the glass and silvered surfaces. Since earlier studies by our laboratories and others have shown that biotinylated BSA readily forms a monolayer on both silver and glass substrates,<sup>38–42</sup> we expected comparable surface binding to

- (12) Whitehead, T. P.; Thorpe, G. H. G.; Carter, T. J. N.; Groucutt, C.; Kricka, L. J. *Nature* **1983**, *306*, 158–159.
- (13) Kricka, L. J. In *Bioluminescence and Chemiluminescence: Fundamental and Applied Aspects*; Campbell, A. K., Kricka, L. J., Stanley, P. E., Eds.; Wiley: Chichester, 1994.
- (14) Feissner, R.; Xiang, Y.; Kranz, R. G. *Anal. Biochem.* **2003**, *315*, 90–94.
- (15) Ozinkas, A. In *Topics in Fluorescence Spectroscopy*; Lakowicz, J. R., Ed.; Plenum Press: New York, 1994; Vol. 4.
- (16) Bange, A.; Halsall, H. B.; Heineman, W. R. *Biosens. Bioelectron.* **2005**, *20*, 2488–2503.
- (17) Hemmilam, L. A. *Applications of Fluorescence in Immunoassays*; John Wiley and Sons: New York, 1992.
- (18) Gosling, J. P. *Clin. Chem.* **1990**, *36*, 1408–1427.
- (19) Davidson, R. S.; Hilchenbach, M. M. *Photochem. Photobiol.* **1990**, *52*, 431–438.
- (20) Vo, Dinh, T.; Sepaniak, M. J.; Griffin, G. D.; Alarie, J. P. *Immunosensors* **1993**, *3*, 85–92.
- (21) Schweitzer, B.; Kingsmore, S. F. *Curr. Opin. Biotechnol.* **2002**, *13*, 14–19.
- (22) Sridar, V. *Indian J. Chem., Sect. B: Org. Chem. Incl. Med. Chem.* **1997**, *36*, 86–87.
- (23) Varma, R. S. Astrazeneca Research Foundation, India, Bangalore, 2002.
- (24) Caddick, S. *Tetrahedron* **1995**, *51*, 10403–10432.
- (25) Lin, J. C.; Yuan, P. M. K.; Jung, D. T. *Bioelectrochem. Bioenerg.* **1998**, *47*, 259–264.
- (26) Akins, R. E.; Tuan, R. S. *Mol. Biotechnol.* **1995**, *4*, 17–24.
- (27) Croppo, G. P.; Visvesvara, G. S.; Leitch, G. J.; Wallace, S.; Schwartz, D. A. *Arch. Pathol. Lab. Med.* **1998**, *122*, 182–186.
- (28) Philippova, T. M.; Novoselov, V. I.; Alekseev, S. I. *Bioelectromagnetics* **1994**, *15*, 183–192.
- (29) Van, Triest, B.; Loftus, B. M.; Pinedo, H. M.; Backus, H. H. J.; Schoenmakers, P.; Telleman, F.; Tadema, T.; Aherne, G. W.; Van, Groeningen, C. J.; Zoetmulder, F. A. N.; Taal, B. G.; Johnston, P. G.; Peters, G. J. *J. Histochem. Cytochem.* **2000**, *48*, 755–760.
- (30) Rhodes, A.; Jasani, B.; Balaton, A. J.; Barnes, D. M.; Anderson, E.; Bobrow, L. G.; Miller, K. D. *Am. J. Clin. Pathol.* **2001**, *115*, 44–58.

- (31) Bismuto, E.; Mancinelli, F.; d'Ambrosio, G.; Massa, R. *Eur. Biophys. J. Biophys. Lett.* **2003**, *32*, 628–634.
- (32) Roy, I.; Gupta, M. N. *Curr. Sci.* **2003**, *85*, 1685–1693.
- (33) Porcelli, M.; Cacciapuoti, G.; Fusco, S.; Massa, R.; d'Ambrosio, G.; Bertoldo, C.; DeRosa, M.; Zappia, V. *FEBS Lett.* **1997**, *402*, 102–106.
- (34) Geddes, C. D.; Aslan, K.; Gryczynski, I.; Malicka, J.; Lakowicz, J. R. In *Topics in Fluorescence Spectroscopy*; Lakowicz, J. R., Ed.; Kluwer Academic/Plenum Publishers: New York, 2005; pp 401–448.
- (35) Geddes, C. D.; Aslan, K.; Gryczynski, I.; Malicka, J.; Lakowicz, J. R. In *Reviews in Fluorescence 2004*; Lakowicz, J. R., Ed.; Kluwer Academic/Plenum Publishers: New York, 2004; pp 365–401.
- (36) Aslan, K.; Geddes, C. D. *Anal. Chem.* **2005**, *77*, 8057–8067.
- (37) Aslan, K.; Maly, S. N.; Geddes, C. D. *J. Am. Chem. Soc.* **2006**, *128*, 13372–13373.
- (38) Wilchek, M.; Bayer, E. A. *Methods Enzymol.* **1990**, *184*, 14–45.
- (39) Wilchek, M.; Bayer, E. A. *Anal. Biochem.* **1988**, *171*, 1–32.
- (40) Green, N. M. *Adv. Protein Chem.* **1975**, *29*, 85–133.

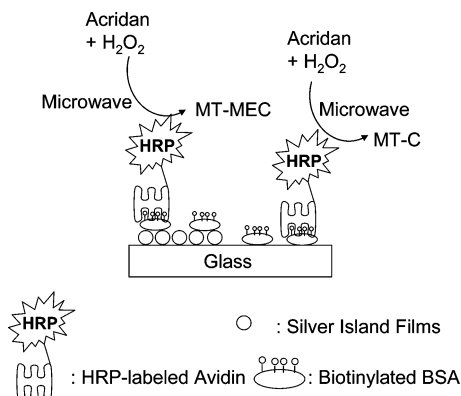


**Figure 1.** HRP–acridan chemiluminescence assay on both glass and silvered slides.

both glass and SiF substrates for a range of BSA–biotin concentrations. As a result, chemiluminescent reaction rates for these experiments are proportional to the quantity of bound biotinylated BSA HRP–streptavidin complexes,<sup>43</sup> where the dynamic range of protein concentration is proportional to the total luminescent photon flux for a defined time interval.

Following surface modification of glass and silver surfaces, we sought to compare traditional chemiluminescence reaction yields with microwave (Mw) “trigger” reaction yields. With the addition of the chemiluminescent mixtures to the functionalized surfaces, we collected the emission data for the MT-MEC assays within the microwave cavity using a fiber optic that is connected to a spectrofluorometer and a computer (not shown). The microwave cavity power was  $\sim 140$  W, which is the same as that utilized in MA-MEF<sup>36</sup> and is of a similar power used for immunostaining.<sup>44,45</sup> Detection was accomplished through a fiber delivered through a small opening on the top of the microwave cavity. Imaging chambers were placed in the microwave, and wells of interest were aligned with the tip of the fiber to optimize collection efficiencies.

Figure 2 top shows the first 500 s of collection time for the chemiluminescence emission from the glass surfaces. Figure 2, bottom, shows the chemiluminescence emission from the glass substrate under the same initial conditions, but the sample is subjected to 30-s microwave pulses at  $\sim 100$ -s intervals. These results clearly show the “on-demand” nature of microwave-triggered chemiluminescence reactions. The most striking feature of Figure 2 is the enhancement of the photon flux upon the application of discrete microwave pulses. In essence, these results demonstrate the feasibility of increasing reaction rates of chemiluminescent reactions and dramatically improving photon flux for finite time intervals. As a result, chemiluminescent reactions that typically generate limited light emission over extended periods of time can be subsequently accelerated with the addition of low-power microwave pulses. In Figure 3, we subsequently demonstrate significant enhancement with microwave pulses from silver island films. Figure 3, top, shows metal-enhanced chemilumines-

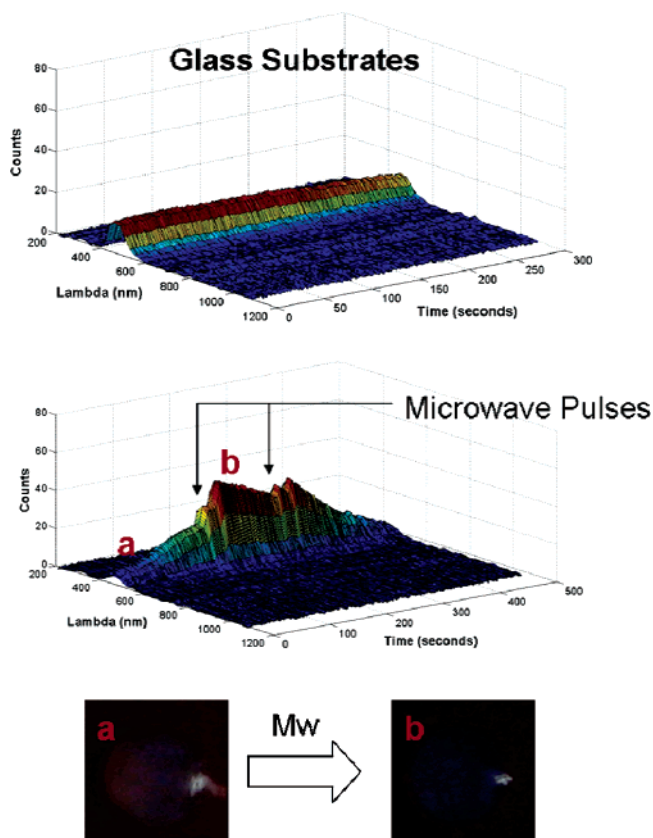


**Figure 2.** 3D plots of acridan assay emission as a function of time from glass slides without (top) and with low-power microwave exposure/pulses (middle). (Bottom) Photographs showing the acridan emission both before (a) and after a low-power microwave pulse (b). Mw, microwave pulse. The concentration of BSA–biotin was 1.56  $\mu$ M.

cence.<sup>46</sup> As compared to the results of Figure 2, top, we notice a pronounced increase in photon flux from the metal surfaces; cf. Figure 2, top, a 3-fold enhancement in signal is observed from the silvered surfaces. These results are further demonstrated with the insets in Figures 2 and 3 that show the real-color photographs of the chemiluminescent reagents (before and after Mw exposure) on glass and the SiF surfaces. When subjected to low-power microwaves as shown in Figure 3, bottom, chemiluminescence from the silver island films is even further enhanced for the microwave pulse time intervals. We believe that the high photon flux that we see upon delivery of microwave pulses to the metal surface is attributed to localized heating of the metal surfaces. The local temperature increase not only accelerates the rate of the chemiluminescence reactions, but the proximity to the silver allows for metal-enhanced chemiluminescence.<sup>46</sup> Thus, a reaction that traditionally is followed over extended periods of time can be “triggered” in short discrete time intervals with low-power microwaves.

The evidence of localized heating of metallic nanoparticles was shown previously.<sup>47</sup> When exposed to weak microwave fields (at 12 GHz), gold colloids absorbed and dissipated the electromagnetic energy *without* any bulk heating, i.e., no water absorption

(41) Lakowicz, J. R.; Geddes, C. D.; Gryczynski, I.; Malicka, J.; Gryczynski, Z.; Aslan, K.; Lukomska, J.; Matveeva, E.; Zhang, J. A.; Badugu, R.; Huang, J. *J. Fluoresc.* **2004**, *14*, 425–441.

(42) Aslan, K.; Holley, P.; Davies, L.; Lakowicz, J. R.; Geddes, C. D. *J. Am. Chem. Soc.* **2005**, *127*, 12115–12121.

(43) Cormier, M. J.; Prichard, P. M. *J. Biol. Chem.* **1968**, *243*, 4706–4714.

(44) Micheva, K. D.; Holz, R. W.; Smith, S. J. *J. Cell Biol.* **2001**, *154*, 355–368.

(45) Petrali, J. P.; Mills, K. R. *Micro Microanalysis* **1998**, 114–115.

(46) Chowdhury, M. H.; Aslan, K.; Malyn, S. N.; Lakowicz, J. R.; Geddes, C. D. *J. Fluoresc.* **2006**, *16*, 295–299.

(47) Kogan, M. J.; Bastus, N. G.; Amigo, R.; Grillo-Bosch, D.; Araya, E.; Turiel, A.; Labarta, A.; Giral, E.; Puntès, V. F. *Nano Lett.* **2006**, *6*, 110–115.

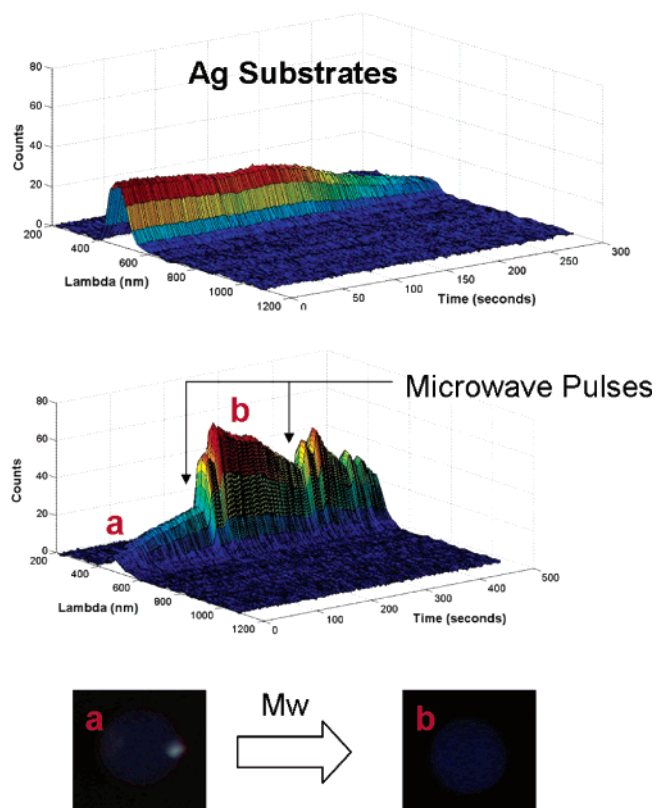


**Figure 3.** 3D plots of the acridan assay chemiluminescence emission as a function of time from silvered glass slides (Ag) without (top) and with low-power microwave exposure/pulses (middle). (Bottom) Photographs showing the acridan emission both before (a) and after a low-power microwave pulse (b). Mw, microwave pulse. The concentration of BSA–biotin was 1.56 pM.

band. This was explained by (1) preferential heating of the gold colloids in the medium that they are in by the electromagnetic fields (inductive heating) and (2) dissipation of the absorbed energy by local heat dissipation. In another report by us,<sup>36</sup> fluorescence resonance energy-transfer studies on proteins in proximity to silver nanoparticles revealed that proteins do not denature when exposed to microwaves (140 W, at 2.45 GHz for 30 s) despite the absorption of electromagnetic energy by water at 2.45 GHz that results in an increase in biomolecular reaction rates, which was attributed to localized heating of the metal surfaces. In the current study, the microwave power settings were similar to those in our previous report,<sup>36</sup> and the observed increase in the chemiluminescent intensity (indicative of reaction rate) is attributed to the localized dissipation of absorbed energy by silver nanoparticles. The microwave heating of the whole sample (SiFs, HRP, and bulk solution) affects the enzyme-catalyzed chemiluminescence reactions in two ways: (1) since the enzyme is only on the surface of the silver nanoparticles, the chemiluminescence reactions only happen on SiFs, and the dissipated energy by SiFs is thought to lower the energy required for these reactions; (2) the heating of the solution increases the diffusion of chemiluminescent species so that the chemiluminescence reactions go faster. Although, the percent contribution of these factors to the overall reaction rate is unknown, we believe the localized heating effect is more dominant.

As controls, we have investigated background signals that result from nonspecific binding of the HRP enzyme to the surfaces

that were not coated with biotinylated BSA (data not shown). In this regard, the background chemiluminescence signal from the glass and metal surfaces treated with only 1% BSA blocking solution and HRP–streptavidin solution was measured. We found that the signal decayed rapidly, which is attributed to the signal generated from the chemiluminescent reaction in the presence of residual HRP enzyme that binds nonspecifically to the substrate. As we have previously shown, the background decay on the silver surfaces is shorter than the decay on glass substrates. These results are consistent with our previous findings that nonspecific background on glass substrates is reduced in the presence of silver island films.

We also sought to demonstrate that the MT-MEC phenomenon is due to the proximity of the assay, by the lack of chemiluminescence enhancement in free solution on both silver island films and glass substrates in the presence of low-power microwaves, i.e., assay not incubated on the surface. We mixed the chemiluminescent reactants and HRP–streptavidin in solution (100  $\mu\text{g}/\text{mL}$ ) to demonstrate that the localized chemiluminescent enhancement in the presence of silver island films is no longer observed. Data were collected for 400 s, and solutions were pulsed with low-power microwaves for 30 s at the 100- and 200-s time points during the course of the reaction. Figure 4, top and bottom, depict a fast signal decay for the reactions in solution above both glass and silver. In addition, upon application of the first microwave pulse, we can see a small signal enhancement, which we believe is due to the few HRP molecules and chemiluminescent reactants that have settled close to the surfaces. For the second microwave pulse, very little signal enhancement is seen and, eventually, no signal observed at longer times. We believe that this result affirms the assertion that preferential heating of the nanostructures by microwaves affords for MT-MEC to be localized in proximity to the silvered surfaces, alleviating unwanted emission from the distal solution.

In order to demonstrate the “on-demand” nature of MT-MEC and induce the higher sensitivity of detection, we varied the amount of biotinylated BSA incubated on the substrate surfaces to demonstrate the concentration dependence for MT-MEC. Figure 5 shows the time-dependent chemiluminescent emission of the chemiluminescence reaction on SiFs and glass surfaces with multiple microwave exposures (four 30-s exposures, 100-s intervals). As previously observed in Figures 2 and 3, the intensity “spikes” correspond to the microwave pulses that trigger enhanced chemiluminescence from the HRP functionalized substrates. Each curve (a–e) corresponds to a different concentration of biotinylated BSA incubated on a silver substrate, recalling that our previous studies have shown monolayer coverage of BSA after incubation.<sup>41,42</sup> From Figure 5, we have been able to determine that the chemiluminescence intensity is proportional to the concentration of HRP bound to BSA-functionalized surfaces. This result is consistent with previously published kinetic studies for the dependence of reaction rates on HRP concentration at fixed concentrations of luminophore-dependent chemiluminescent reactants.<sup>43</sup> This enables the surface protein concentration to be determined.

It is important to explain the characteristics of the chemiluminescent intensity versus time plot, Figure 5, in detail and the method we have used them for calibration and determination of

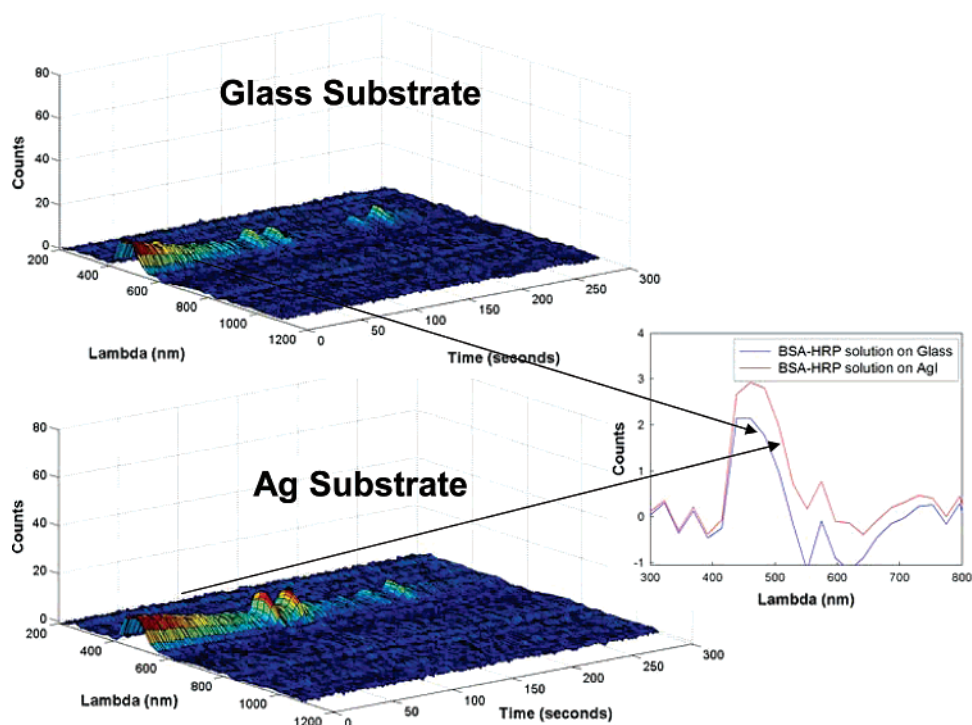


**Figure 4.** 3D plots of the acridan assay chemiluminescence emission from both glass (top) and silvered substrates (bottom). (Right) Emission spectra are the average of 400 1-s time points. In both cases, BSA–biotin was *not* immobilized to the surfaces, which were exposed to microwave pulses at 100- and 200-s time points. The final concentration of HRP–streptavidin in the assay was  $\sim 10 \mu\text{g/mL}$ .

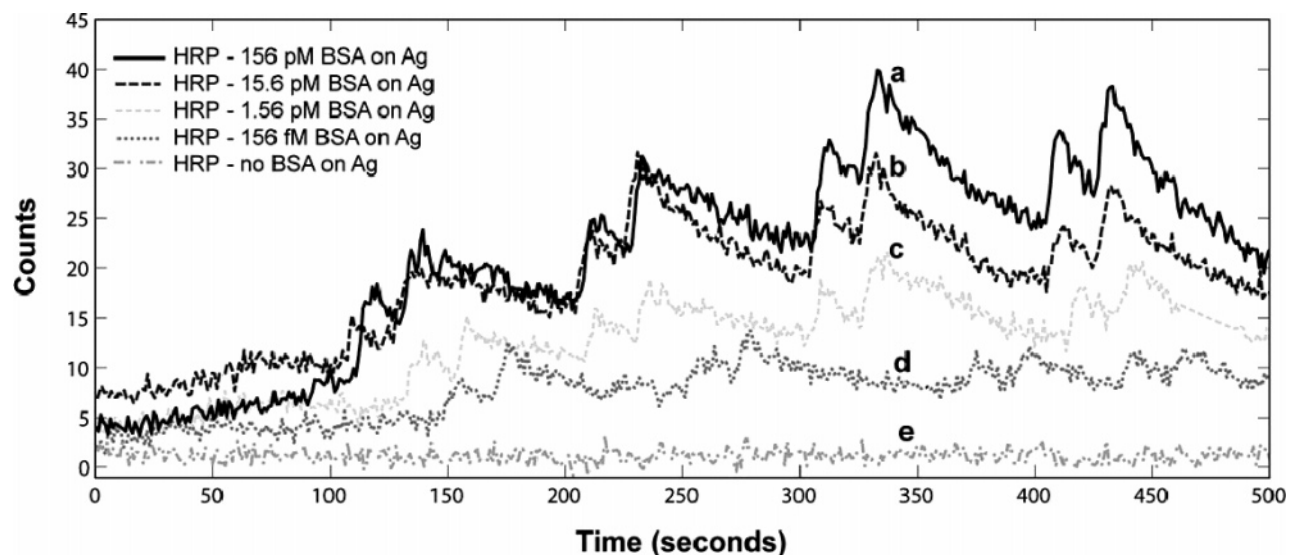


**Figure 5.** Acridan chemiluminescence emission intensity as a function of time for different concentrations of surface-bound BSA–biotin. a, 156 pM BSA–biotin; b, 15.6 pM BSA–biotin; c, 1.56 pM BSA–biotin; d, 156 fM BSA–biotin; and e, no BSA–biotin.

surface protein concentration. First, in order to determine the concentration of surface proteins without microwave heating, the change in chemiluminescent intensity was monitored after the chemiluminescent reactions were initiated (no microwave heating) in the first 100 s. It is seen that, without microwave heating, the chemiluminescent intensity is slightly increased as the concentration of BSA is increased but little difference between them is observed, which proved to be a not useful method. On the other hand, to show the benefits of microwave heating to increase the detected chemiluminescent signal, four 30-s exposures (after 100 s) were performed with 100-s intervals to drive the chemiluminescent reactions to completion within 400 s (without microwave

heating the reactions studies here are completed longer than 30 min<sup>46</sup>). The photon flux (in counts), area under the intensity–time plot, is an indication of the extent of the HRP-catalyzed reaction and thus provides information about the presence of surface-bound BSA. The two “peaks” seen after each microwave exposure, in Figure 5, are a result of the microwave magnetron pulsing. During the 10- and 5-s runs, the chemiluminescent intensity increases and decreases, respectively triggered by the magnetron pulsing and the localized heating of the microwaves. The peak height and the area under one of the peaks could be increased by using shorter exposure times (<10 s) and higher initial microwave power settings. However, we found that higher

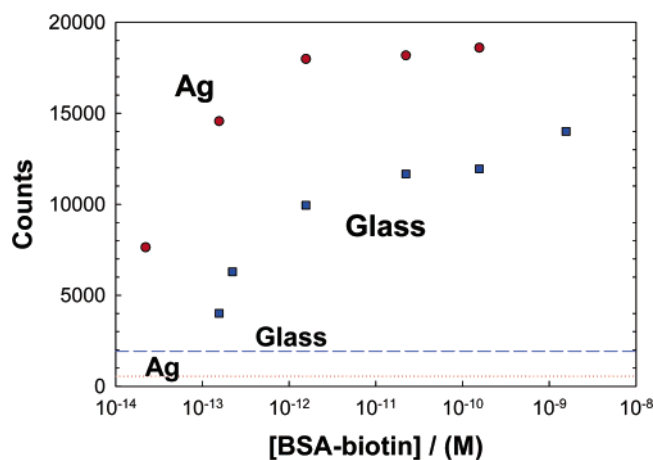


**Figure 6.** Photon flux integrated over 500 s of the assay shown in Figure 5, for different concentrations of BSA–biotin from both glass and silvered surfaces (Ag). Baselines correspond to integrated photon flux over 500 s for glass and silvered surfaces (Ag) incubated with 1% BSA solution and streptavidin HRP.

initial power setting causes surface drying and was not found reliable for use here, as surface drying causes protein denaturation. In all the experiments performed with low-power microwaves, using both SiFs and glass, there was no evidence of surface drying. This is attributed to the previously made observations<sup>36</sup> that the temperature increase of the aqueous solution on the surfaces due to microwave heating is only  $\sim 8$  °C (to  $\sim 28$  °C) for 30  $\mu$ L of aqueous sample.<sup>36</sup>

It is also important to comment on the reproducibility of the MT-MEC technique for quantitative detection of proteins as the accuracy of the proposed method mostly depends on microwave heating, while the precision of the technique depends on other minor factors such as the SiFs, substrates, etc. The reproducible preparation of SiFs has been addressed before<sup>42,46,48–50</sup> and is highly reproducible. The chemiluminescent reactions are also well-established and are most widely used in commercially available chemiluminescent kits. As indicated in the Experimental Section, the microwave source used in this study has a standard 2.45-GHz magnetron and is used in commercially available microwave ovens. The MT-MEC technique we describe here takes advantage of the use of these commonly available well-established tools, together resulting in the reproducible and fairly simple quantitative detection of surface proteins.

It is interesting to compare the results of the protein concentration-dependent assays on both silvered and glass surfaces, Figure 6. The overall signal enhancement shown in Figure 5, for assays performed on silver substrates versus those on glass substrates, serves to confirm the benefits of using silver nanostructures for MEC. By combining the use of low-power microwaves and metal substrates to increase the rapidity of streptavidin binding to biotinylated BSA surfaces, decrease nonspecific background, and enhance and accelerate chemiluminescent reactions, we demonstrate in Figure 6 that we can indeed detect approximately femtomoles of biotinylated BSA on surfaces in less

than 2 min, with a signal-to-noise ratio (S/N) greater than 8. Signal-to-noise ratio is obtained from Figure 6, and is equal to the ratio of the lowest counts (y-axis) obtained using HRP divided by the counts without HRP (horizontal lines): for Ag,  $S/N = 7200/900$  counts  $> 8$ . With these results, we predict that this application can be generally applied to both detect and quantify a great many other biomolecules as well. As compared to traditional western blot approaches, Figure 7, MT-MEC offers protein quantification with ultrafast assay times, i.e.,  $< 2$ -min total assay time versus  $\sim 80$  min.

## CONCLUSIONS

Using low-power microwaves, we have demonstrated an inexpensive and simplistic approach to overcome some of the classical physical constraints imposed by current protein detection platforms, namely, assay rapidity, sensitivity, specificity, and accurate protein quantification.<sup>15–21</sup> With the MT-MEC approach, we have shown that the sensitivity of detection ( $< 0.5$  pg) is 1 order of magnitude greater than that available with currently standard commercially available methodologies (i.e., ECL Plus Western Blotting Detection Kit, RPN2132, Amersham Biosciences). In addition to the improved detection sensitivity, we have demonstrated that these assays can be performed in a fraction of the time (in fact, less than 1 min) typically required with standard methodologies. Further improvement is likely required with the addition of microwave steps to the initial protein incubation and blocking steps. With the application of microwaves and the subsequent acceleration of the chemiluminescent reaction, the on-demand nature of light emission not only increases the detectability of low concentrations of proteins, but photon flux is also proportional to the concentration of the protein on a surface. Thus, for a defined time interval, we are able to accurately quantify surface protein. For immunoassays in the clinical setting, the MT-MEC approach offers a potentially powerful approach to protein detection because it substantially decreases current assay times to minutes, potentially decreases false positives due to increased specificity, and increases assay sensitivity by at least 1 order of magnitude (see Figure 6). In addition, we believe that the MT-MEC approach offers the following benefits:

1. HRP both catalyzes and positions the reactants close to silver for metal-enhanced chemiluminescence<sup>46</sup> as well as for microwave heating.
2. As we have shown in Figure 4, the material distal from the metal contributes little to the total assay photon flux.
3. The chemiluminescence assay/reactants can be depleted using microwave pulses in less than 1 min; however, we envision much quicker times may be realized by implementing high microwave irradiances and ordered surface bound nanostructures.
4. While we have shown a detectability limit of  $\sim 150$  fM protein with a signal to noise ratio of  $> 8$  in less than 1 min, we believe that by using more suitable silvered immobilized nanostructures that our detectability would be significantly lower. For example, silver nanorods and triangular surfaces have shown  $> 50$ -fold enhancements of fluorescence,<sup>51,52</sup> whereas fractal surfaces have shown  $> 3000$ -fold enhancements.<sup>53–55</sup> Since, these structures may

(48) Aslan, K.; Holley, P.; Geddes, C. D. *J. Immunol. Methods* **2006**.

(49) Aslan, K.; Lakowicz, J. R.; Szmajcinski, H.; Geddes, C. D. *J. Fluoresc.* **2005**, *15*, 37–40.

(50) Aslan, K.; Leonenko, Z.; Lakowicz, J. R.; Geddes, C. D. *J. Fluoresc.* **2005**, *15*, 643–654.

(51) Aslan, K.; Leonenko, Z.; Lakowicz, J. R.; Geddes, C. D. *J. Phys. Chem. B* **2005**, *109*, 3157–3162.

(52) Aslan, K.; Lakowicz, J. R.; Geddes, C. D. *Anal. Bioanal. Chem.* **2005**, *382*, 926–933.

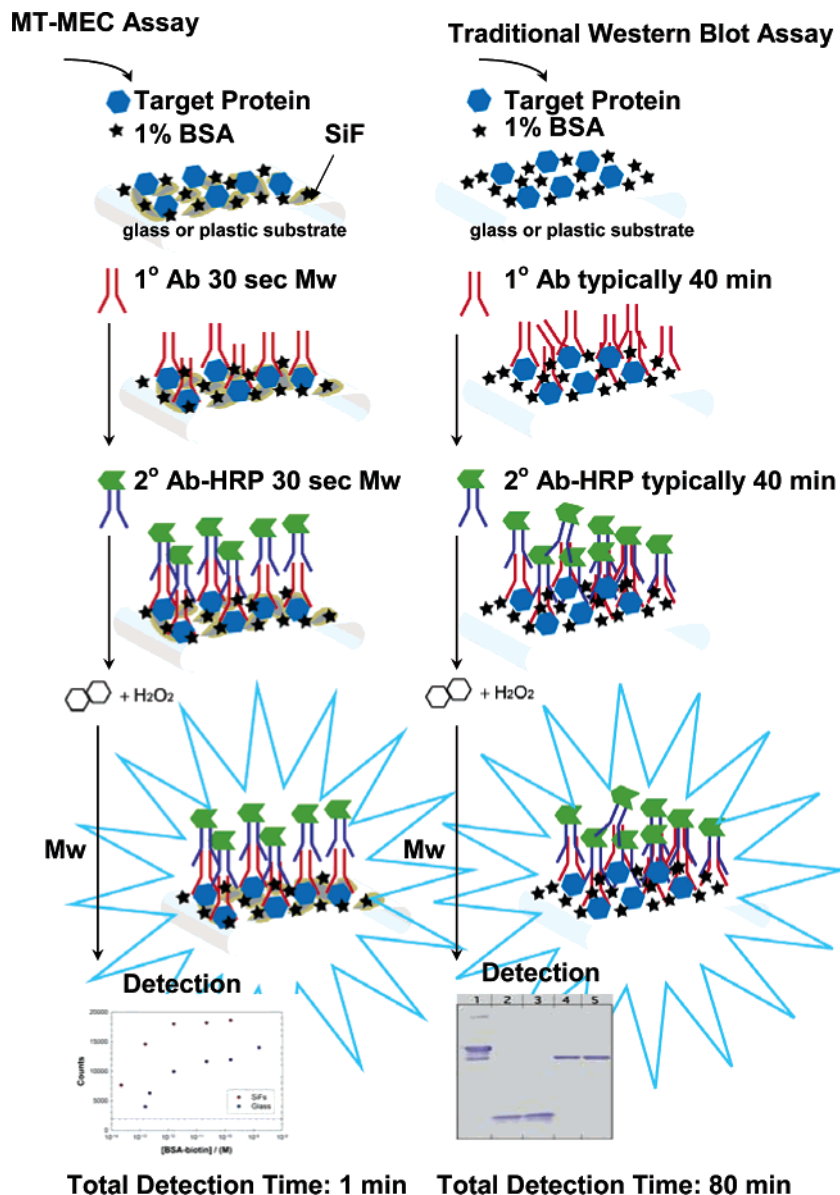


**Figure 7.** Procedure for the MT-MEC immunoassay (Mw, low-power microwave heating).

absorb/dissipate more energy when heated with microwaves due to their highly concentrated electric fields around the edges, we expect the chemiluminescent reactions to be completed much quicker.

5. A whole range of anchor proteins and associated chemistries are available to anchor the detection protein to the silvered surfaces. In addition, we have recently shown the applicability of MEF from modified plastic substrates, which could also be used in this regard<sup>56</sup> as an alternative to nitrocellulose to transfer gel-separated proteins.

6. With the decreased reaction times, increased sensitivity, increased specificity, and signal enhancement achieved with MT-

MEC, we have also dramatically *decreased* the volume of reagents required to perform these assays. Thus, we anticipate that implementing MT-MEC into standard protein detection methodologies will decrease reagent waste and overall experimental costs. With this technology, both ultrafast and ultra bright chemiluminescence assays can be realized.

## MATERIALS AND METHODS

**Materials.** Bovine-biotinamidocaproyl-labeled albumin (biotinylated BSA), HRP-labeled avidin, silver nitrate (99.9%), sodium hydroxide (99.996%), ammonium hydroxide (30%), trisodium citrate, D-glucose, and premium quality APS-coated glass slides (75 × 25 mm) were obtained from Sigma-Aldrich. CoverWell imaging chamber gaskets with adhesive (20-mm diameter, 1 mm deep) were obtained from Molecular Probes (Eugene, OR). Streptavidin–HRP prediluted solution was obtained from Chemicon International Inc. Chemiluminescence materials were purchased from Amersham Biosciences (ECL Plus Western blotting detection kit, RPN2132). ECL Plus utilizes a new technology, developed

(53) Geddes, C. D.; Parfenov, A.; Gryczynski, I.; Malicka, J.; Roll, D.; Lakowicz, J. R. *J. Fluoresc.* **2003**, *13*, 119–122.

(54) Geddes, C. D.; Parfenov, A.; Roll, D.; Gryczynski, I.; Malicka, J.; Lakowicz, J. R. *J. Fluoresc.* **2003**, *13*, 267–276.

(55) Parfenov, A.; Gryczynski, I.; Malicka, J.; Geddes, C. D.; Lakowicz, J. R. *J. Phys. Chem. B* **2003**, *107*, 8829–8833.

(56) Aslan, K.; Badugu, R.; Lakowicz, J. R.; Geddes, C. D. *J. Fluoresc.* **2005**, *15*, 99–104.

by Lumigen Inc., based on the enzymatic generation of an acridinium ester, which produces intense light emission at  $\sim 430$  nm.

**(1) Formation of Silver Island Films on APS-Coated Glass Substrates.** In a typical SiF preparation, a solution of silver nitrate (0.5 g in 60 mL of deionized water) in a clean 100-mL glass beaker, equipped with a Teflon-coated stir bar, is prepared and placed on a Corning stirring/hot plate. While stirring at the quickest speed, 8 drops ( $\sim 200 \mu\text{L}$ ) of freshly prepared 5% (w/v) sodium hydroxide solution are added. This results in the formation of dark brown precipitates of silver particles. Approximately 2 mL of ammonium hydroxide is then added, drop by drop, to redissolve the precipitates. The clear solution is cooled to  $5^\circ\text{C}$  by placing the beaker in an ice bath, followed by soaking the APS-coated glass slides in the solution. While keeping the slides at  $5^\circ\text{C}$ , a fresh solution of D-glucose (0.72 g in 15 mL of water) is added. Subsequently, the temperature of the mixture is then warmed to  $30^\circ\text{C}$ . As the color of the mixture turns from yellow-green to yellow-brown, and the color of the slides become green, the slides are removed from the mixture, washed with water, and sonicated for 1 min at room temperature. SiF-deposited slides were then rinsed with deionized water several times and dried under a stream of nitrogen gas. Prior to assay fabrication and subsequent chemiluminescent experiments, imaging chamber gaskets with adhesive (20-mm diameter, 1 mm deep) were pressed against the silver-coated and silica-capped microscope glass slides until they were stuck together, creating a chamber.

**(2) Preparation of the Model Protein Assay (Biotin–Avidin) on Silver Island Films and on Glass.** The model assay used in this paper is based on the well-known interactions of biotin and avidin. Biotin groups are introduced to the glass and silvered surfaces through biotinylated BSA, which readily forms a monolayer on the surfaces of glass and SiFs.<sup>38–40</sup> Biotinylated BSA is bound to SiFs and the glass by incubating  $20 \mu\text{L}$  of biotinylated BSA solutions with different concentrations in the imaging for  $\sim 1$  h. Chambers were washed with water to remove the unbound material. Imaging chambers were then incubated with  $20 \mu\text{L}$  of 1% aqueous BSA (w/v) for 1 h to minimize nonspecific binding of HRP–streptavidin to surfaces. Chambers were again washed with water to remove the BSA blocking solution. Stock solutions of HRP–streptavidin were diluted 1:10 to a final concentration of  $100 \mu\text{g}/\text{mL}$ . Twenty microliters of the HRP–streptavidin solution was subsequently added into the biotinylated BSA-coated glass and SiF-coated imaging chambers and typically microwaved for 20 s in the microwave cavity ( $0.7 \text{ ft}^3$ , GE compact microwave model JES735BF, max power 700 W). The power setting was set to 2, which corresponded to 140 W over the entire cavity, which is similar to that used in our recent finding that low-power microwaves minimize nonspecific binding and incubation times.<sup>57</sup> In all the experiments performed with low-power microwaves, there was no evidence of surface drying. Following incubation, imaging

chambers were again washed with water to remove unbound HRP–streptavidin material prior to the chemiluminescence experiments.

**(3) Chemiluminescence Reagents.** The ECL Western blotting detection kit contained two reagents that yield a bright chemiluminescent emission at 430 nm upon mixing. Solution A contained the substrate solution (peroxide formulation), and solution B contained the solution of the luminescent compound, acridan in dioxane and ethanol. HRP and hydrogen peroxide solution (solution A) catalyze the oxidation of the acridan substrate (solution B). As a result, acridinium ester intermediates are formed and further react with peroxide to generate light emission with a maximum wavelength centered around 430 nm.

**(4) Chemiluminescence from Reagents on SiFs and Glass Surfaces.** The chemiluminescence experiments were performed with and without microwave heating inside the microwave cavity. During microwave heating, 30-s pulses were applied at three 100-s intervals. The pulses were applied at 30% power, which corresponded to 210 W over the entire cavity. In order to obtain the same initial chemiluminescence emission for all measurements, all chemiluminescent assays were undertaken by combining  $40 \mu\text{L}$  of solution A with  $2.0 \mu\text{L}$  of solution B and immediately adding the entire solution to the imaging chamber. Data collection commenced immediately following addition of reagents and terminated when the photon count returned to baseline. Since the rate of photon emission is directly proportional to enzyme concentration, we sum the photon flux for a fixed time interval for the points shown in Figure 3 to determine the relationship between protein concentration and signal intensity, cf. Figures 6 and 7.

**(5) Chemiluminescence Detection.** Chemiluminescence spectra were collected using an Ocean Optics spectrometer, model SD 2000 (Dunedin, FL), connected to an Ocean Optics 1000-mm-diameter fiber with an NA of 0.22. The fiber was positioned vertically on top of the slides containing the chemiluminescent reagents inside the microwave cavity. Chemiluminescent spectra and time-dependent emission intensities were collected with an integration time of 1000 ms for  $\sim 500$  s unless otherwise noted. The integration time was kept constant between the control and silver island film sample measurements.

The *real-color* photographs were taken with an Olympus Digital camera (C-740, 3.2 Mega Pixel,  $10\times$  Optical Zoom) without the need for optical filters.

## ACKNOWLEDGMENT

National Center for Research Resources, RR008119 and salary support to authors from UMBI is acknowledged.

Received for review June 27, 2006. Accepted September 21, 2006.

AC061161+

(57) Aslan, K.; Geddes, C. D. *J. Fluoresc.* **2006**, *16*, 3–8.